4.2 VALLES MARINERIS

4.2.1 Ganges Chasma

The Ganges (7°S/312°E) and Capri Chasmata (9.8°S/316.7°E) are assumed to be the source regions of Simud and Tiu Valles, which are Hesperian-aged outflow channels. Ganges Chasma is situated in the northeastern part of Valles Marineris, north of Capri Chasma and west of Aurorae Chaos (Fig. 2, 10, 28).
Ganges Chasma features five ILDs (Fig. 52) that differ in shape and, in certain parts also in morphology. There are some blocky mesas that resemble similarities to ILDs in chaotic terrains. Dark-toned chaotic terrain remnants as well as dark aeolian material – partially accumulated in dunes - surrounds the ILDs that are exposed on the canyon floor or hillside within a distance of ~330 km.

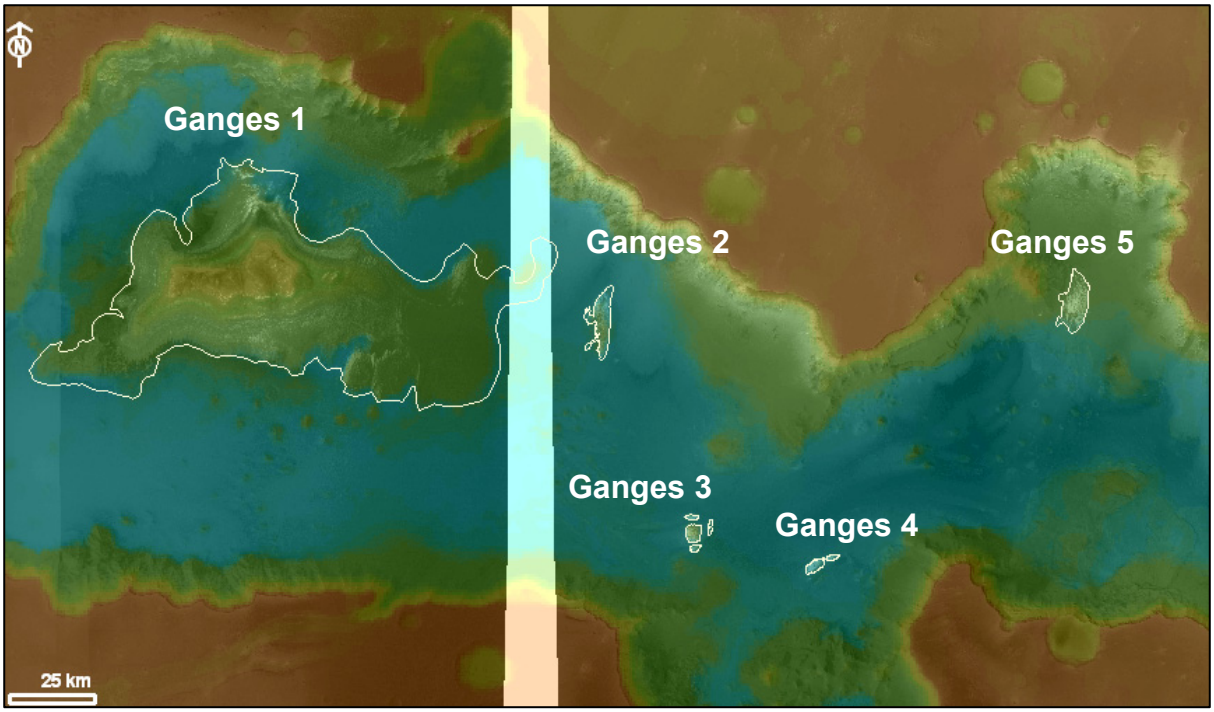

Figure 52: Ganges Chasma ILDs. Mosaic of HRSC orthoimages (orbits h0061_0008, h2222_0000, h2211_0000, h2942_0001, h2178_0000, h2145_0000, h2156_0000) overlain by MOLA DEM (centred at 7°S/313°E).

Ganges 1:

Ganges Mensa (7.0°S/311°E; Fig. 28) features sub-horizontal layering (Fig. 53J) and the typical mesa morphology; it is flat-topped with steep slopes (Fig. 53D) and sprouts wing-like extensions (Fig. 52). As it is situated in the westernmost part of a semi-open chasma, its shape is not streamlined but elongated parallel to the chasma, indicating a correlation to regional tectonics (Fig. 10, 2). The western part of the ILD seems more eroded than the eastern part, which possibly indicates that erosion was more affective from the west. The ILD is exposed between -4100 m and -500 m (Table 17) and measures 180 by 75 km. It shows landslide material all around indicating destabilised slopes.
The ILD is characterised by the parameters shown in Table 17.

It features freshly-eroded cliff-forming material of high albedo and an apparently a more slope-forming material in between (e.g. Fig. 53B, 53D), which is indicated by the stair-stepped morphology. Its high surface temperatures (Fig. 53A) and TI (Sect. 3.2.2, Table 17) suggest that consolidation is more advanced than in surrounding materials, especially in the lower part (Fig. 53I). Accumulations of dark aeolian material cover the flat parts which show lower BTs (cf. 53A, 53D). Its stair-stepped morphology indicates that its materials differ in their resistance to erosion and weathering, alternating between greater and lesser consolidation (Fig. 53D, 53I).
The overall relative albedo is intermediate (Sect. 3.2.1, Table 17) but clearly varies within the ILD (Fig. 53B).
One unit was identified (Fig. 53H, 53D, 53I) but there apparently is another more incompetent and eroded indicated by stair-stepped morphology (Sect. 5.1). One apparently is cliff-forming, while the other one is more slope-forming. The cliff-forming unit features high albedo and gradients and alternates with the low albedo slope-forming unit, resulting in a stair-stepped morphology (Fig. 53B, 53D). Obviously, these units differ in their resistance to weathering and erosion, which is confirmed by TI and BT (Fig. 53A, 53I). The cliff-forming unit in parts exhibits small low-albedo mesas on its surface indicating erosion (cf. Sect. 4.1.1, 4.1.2).
Undulated strata are observed throughout the whole ILD (53C, 53J). Flatter parts seem coarser, which could be a grain-size effect or caused by rock break-up due to more effective weathering. The lower part of the ILD appears extremely finely layered, especially the southern part, which may be due to its steepness, as it is hardly covered by dark aeolian material. Furthermore, the flat parts show even, smooth-looking surfaces which appear disintegrated. There, surface vugs reveal underlying strata in sites not covered by windblown material.
Advanced weathering can be observed throughout the whole ILD, as indicated by visible rock fragmentation. The TI (Fig. 53I) observed in the lower, steep, freshly eroded unit (400-600 SI) is higher than in the upper unit (300-500 SI). Additionally, the upper unit exhibits windblown material that may be thick and dominant enough a (Sect. 3.2.2) to reveal the TI of loose, fined grained material (cf. Sect. 3.2.2). The surface features yardangs, flutes and grooves (Sect. 2.3.1, 5.1), probably the effect of heavy erosion by wind and/ or water (Sect. 2.3.1). The low TI in the upper part and in the flatter regions (on bedding planes; Fig. 53D) is apparently is due to thick low-albedo coverings of aeolian material, which make the top appear smooth (Fig. 53G). Talus and boulders are observed at steep scarps and indicate rock break-up resulting in meter-sized boulders and fine talus.
CRISM and OMEGA observations show that the lower unit of the ILD has a strong kieserite signature [*Mangold et al.,* 2007; *Roach and Mustard*, 2008]. This signature appears in the steep lower parts that show higher TI (Fig. 53I) and BT (Fig. 53A). The windblown dark material on its surface shows no olivine, pyroxene, or ferric oxide spectral signatures (Fig. 53F). This kieserite-rich unit (Fig. 53B) is approximately 1600 m thick when assuming no other mineral phases in between. A transition zone characterized by a discrete layer at an elevation of about -1900 m marks the beginning of the unit (Fig. 53A-D), in which a weak polyhydrated sulphate (PHS) signature was observed by CRISM (Fig. 53G); *Roach and Mustard*, 2008). The dark ripples on top and in grooves show a clinopyroxene (HCP) signature. This mineralogy might correlate with the steepness of the

slopes as observed by *Mangold et al.* (2007) and *Roach et al.* (2008), for kieserite is exposed in the steeper parts and PHS in the less steep parts (Fig. 53D). PHS were detected near the top of the ILD at the elevation of ~-500 m (Fig. 53G).
Although one of these transition zones coincides with the upper kieserite boundary, it is not known whether the lower unit consists entirely of kieserite. As in other ILD regions, such as E-Candor Chasma [*Roach et al.*, 2007], strata of the two sulphates may alternate here. Detection is often hampered by loose material covers. Besides, other minerals that are spectrally neutral may also be involved (Sect. 3.2.2). Sparse haematite deposits were found off the south flank of the ILD in a low albedo material [*Christensen et al.*, 2001b].
High DTMs were used to measure the thickness of boundary layers that are visible in HRSC-data (Fig. 53K, 53H). These boundary layers represent the high-albedo, cliff-forming material that was identified (Fig. 53D, 53K). Five sequences with varying thicknesses were distinguished. Altogether, they comprise a thickness of ~2500 m thick (Fig. 53H); the average thickness per sequence is 500 m. Sequences have been mapped and a profile (Fig. 53K) was generated from their lengthwise layering.
The strike and dip of the layers is shown in Fig. 53J. Layering is assumed sub-horizontal since less than 10° and when regarding the accuracy.

Table 17: Parameters of Ganges 1.

Morphology	Relative Albedo	Elevation [m]	Thickness [m]	Consolidation of Materials	Mineralogy	Layer Geometry
Mesa,; dome-like profile	Intermediate	-4100±12.5 to -500±12.5	3600±12.5 Stair-steps of 500 m	Intermediate TI TI Ø: 424 SI±86 (surrounding: 327 SI±90) BT: 180-198 K (surrounding: 180-185 K) talus and boulders present	Kieserite in the lower part to -1900 m, PHS near the top at ~-500 m; haematite below kieserite	4±2/4±3° below 9±5/255±36

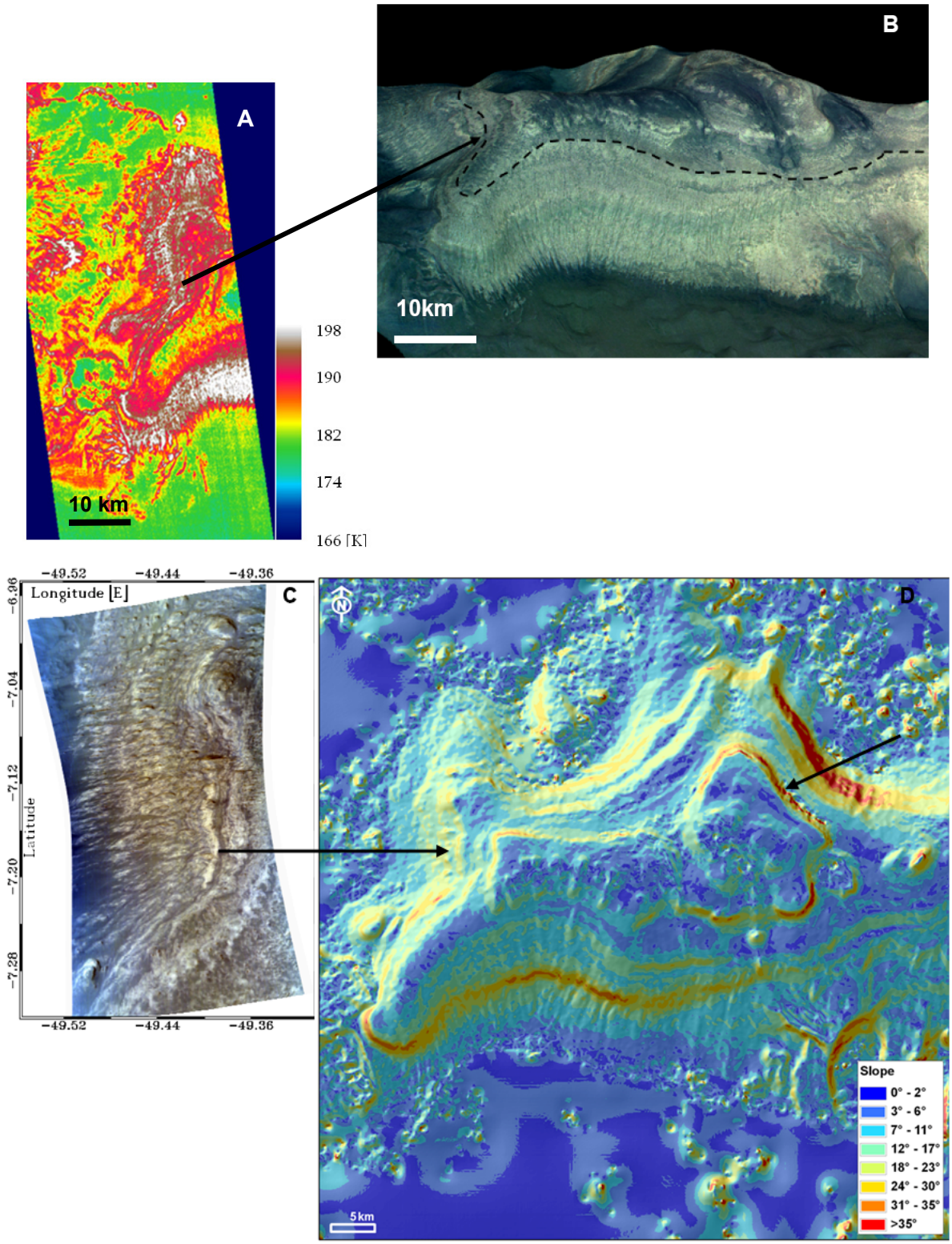

Figure 53: Properties of Ganges 1. (A) THEMIS-BT map (I0706003; L_S = 7.5 →S-fall; 7.6°S/309.6°E) showing high surface temperatures in steep resistant layers. The black arrow marks the boundary below which kieserite was detected (cf. Fig. 53B-D). (B) HRSC false colour image in perspective view (orbit h2211_0000; 7°S/311°E). Ganges Mensa is the ILD with the most distinct layering showing high albedo differences that are due to dark aeolian material coverage (often in ripples) which covers the surface and very flat parts, simulating light and dark layers. The mineralogical signatures of the lower part and top differ as kieserite is observed in the lower part and PHS on the top. The transition zone is marked by a black arrow and a dotted line. Freshly eroded regions feature higher surface temperatures (Fig. 53A) and steeper slopes (>25°; Fig. 53D). (C) Spectral differences visible in a CRISM image (orbit HRL0000633F). Resistant relief-forming light-toned layers (arrow) differ from more smooth-appearing brown layers possibly dust covered. This resistant

unit corresponds to eroded cap rock. The whole lower western region exhibits a strong kieserite signature [*Roach and Mustard*, 2008]. Dark aeolian material is blue. (D) HRSC slope map (orbit h2211_0000) showing steep slopes (>25°) coloured yellow and red, higher surface temperatures (Fig. 53A), higher TI (Fig. 53I) and different resistance to weathering. Steep parts also correspond to the area of the thickness measurement (Fig. 53K).

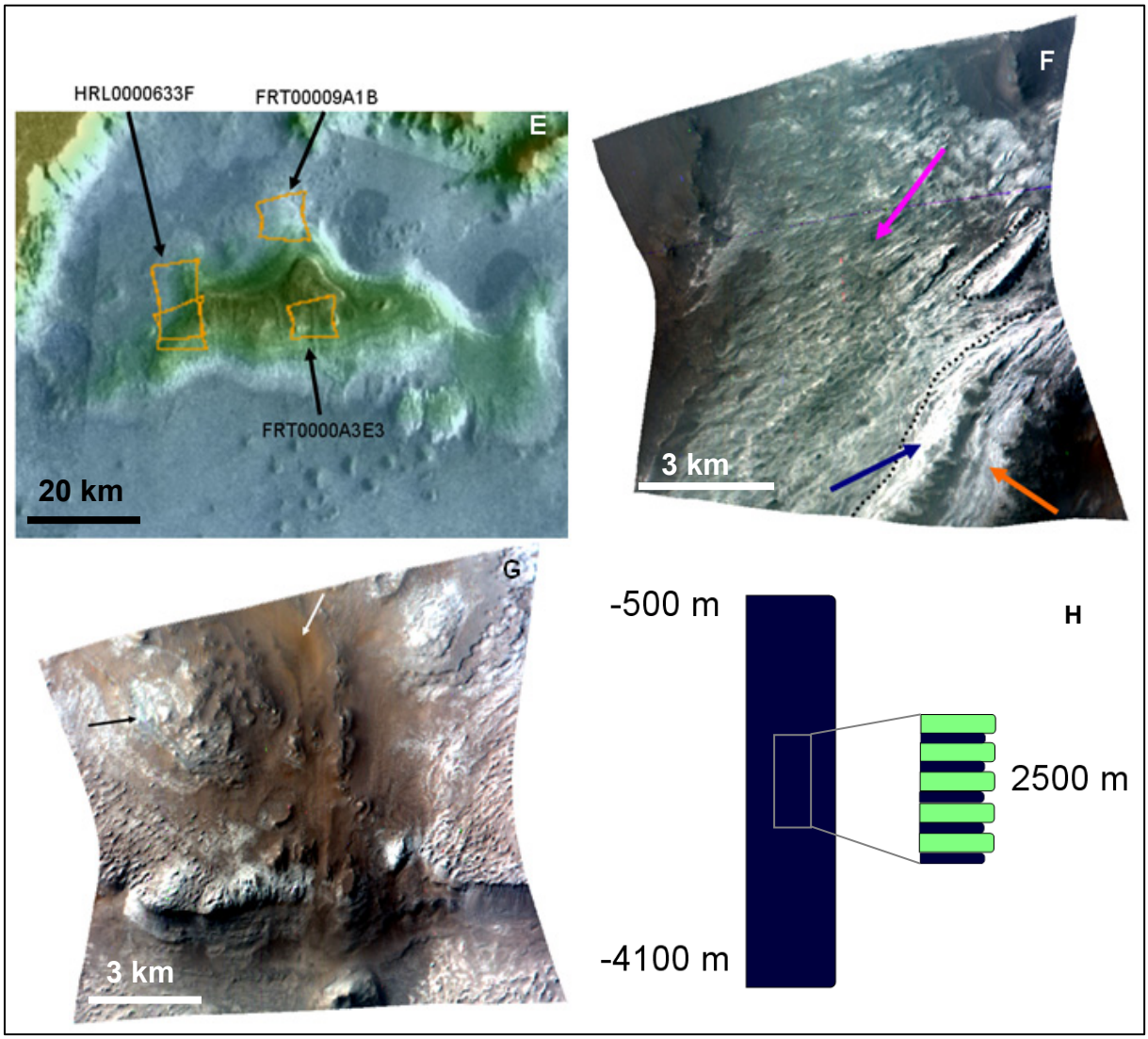

(E) CRISM observations in a MOLA overview (cf. Fig. 53F, 53G). (F) CRISM observation FRT00009A1B (7.6°S/309.6°E). The lowermost part of the ILD features kieserite. The spectral character of kieserite is different in the lower NW and the upper SE part, marked by the dotted line (cf. Fig. 53A-D). Dark areas represent aeolian material that is mostly rippled but neither shows pyroxene, Fe-oxide nor olivine signatures. Arrows mark the regions where spectra were collected [*Roach and Mustard*, 2008]. (G) CRISM observation (orbit FRT0000A3E3; 7°S/311°E) showing the central top of the ILD with HCP-rich (Sect. 3.2.2) ripples (white arrow). The bright ILD material has a PHS signature possibly weakened by aeolian coverage. Kieserite was not observed near the top. (H) Thickness profile showing ILD is exposed between -4100 to -500 m. Within 2500 m, five stair-stepped sequences are exposed (cf. Fig. 53K).

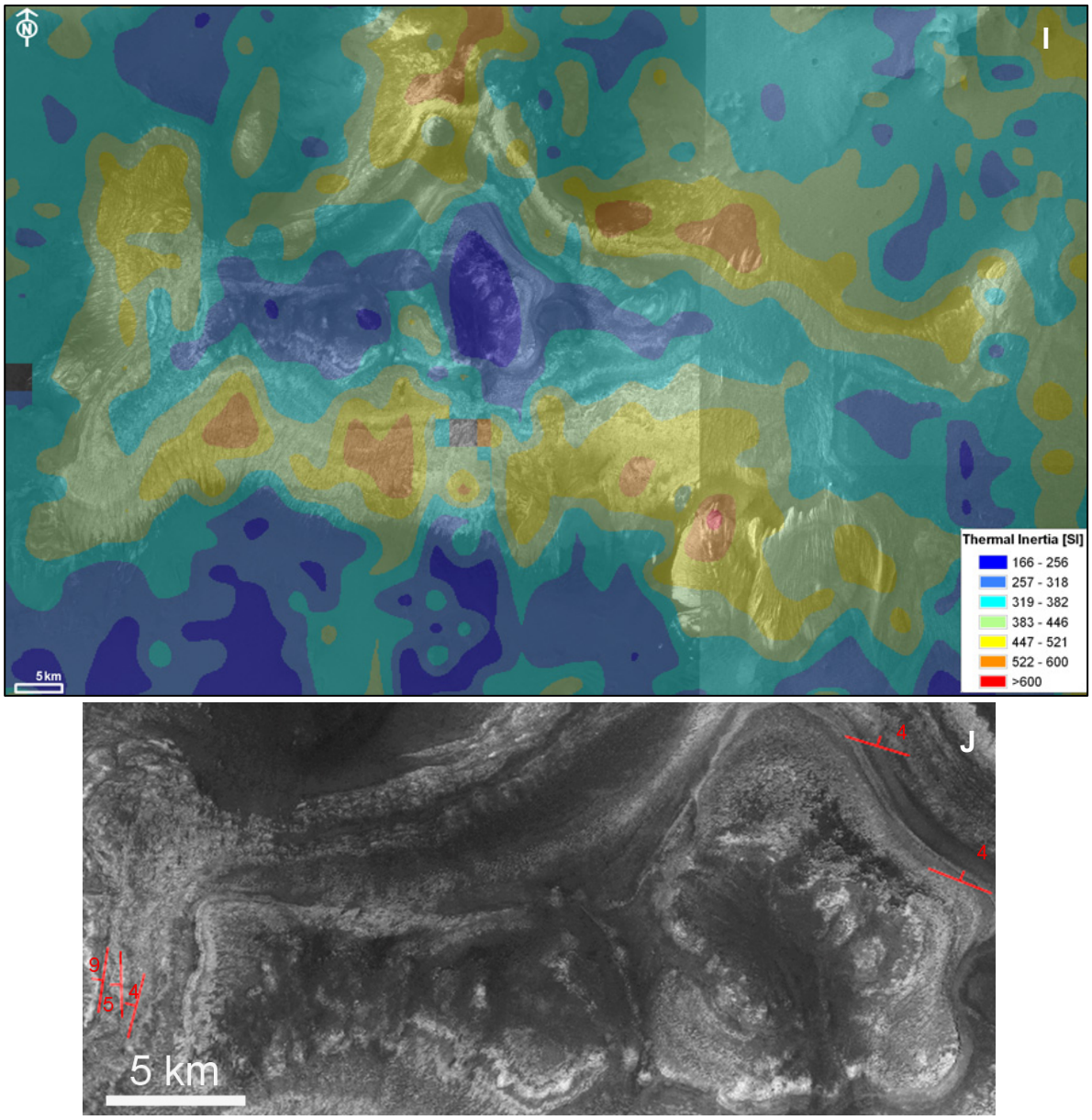

(I) TI map of Ganges Mensa (7°S/311°E). High TI (~600 SI) was observed in the lower, steeper part of the ILD that shows kieserite (cf. Fig. 53B-D); lower values are observed (~400 SI) above where there is more cover of loose material (cf. 53A, 53G). (J) Strike and dip measured in Ganges 1 (7°S/311°E). Layering is sub-horizontal (< 10°) and nearly comparable in the lower and upper parts. The lower part is slightly more inclined. Layers dip downslope, but readings are so low it is impossible to identify outward dipping, which could indicate a volcanic origin (Sect. 3.2.3).

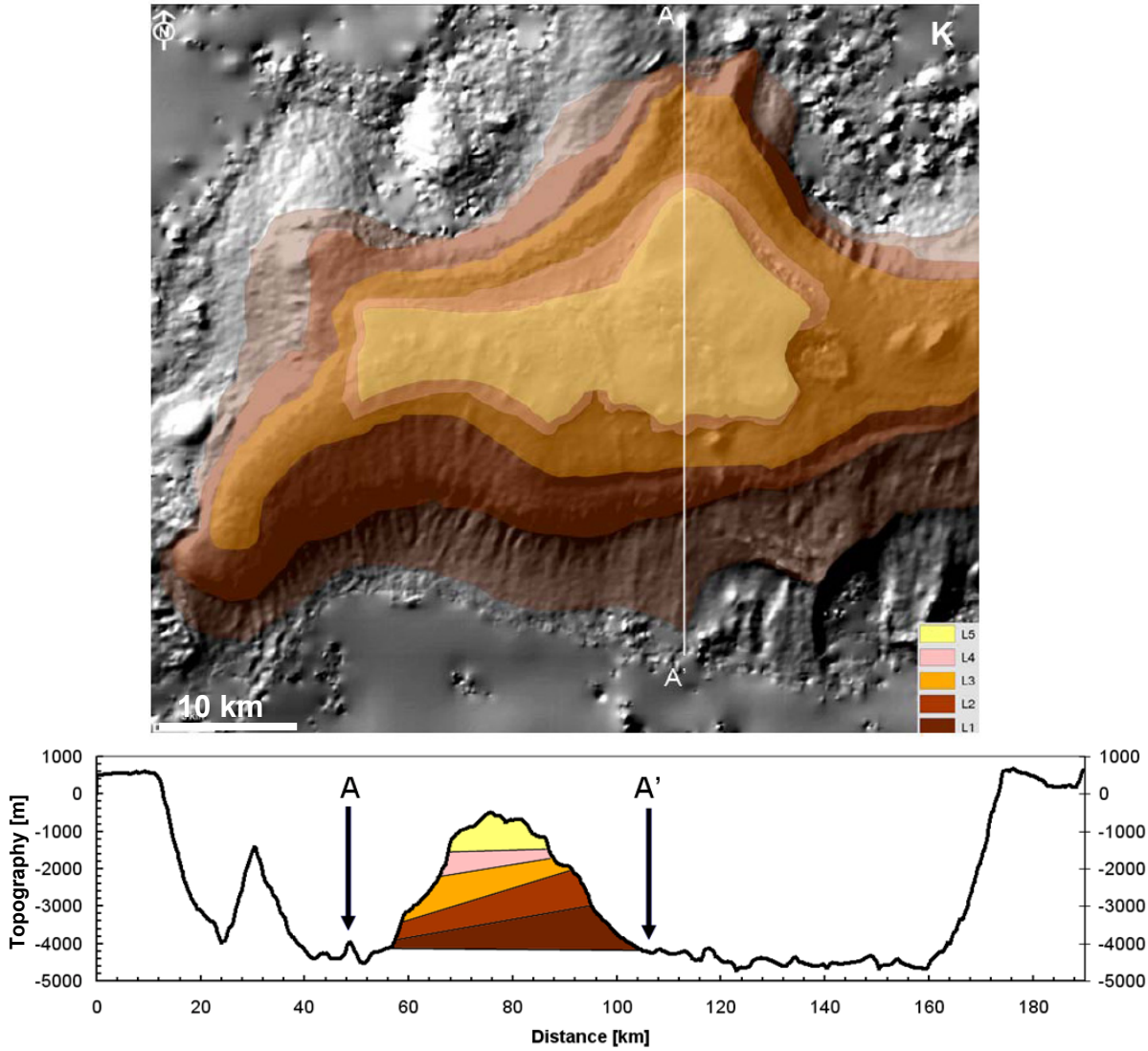

(K) *(top)* HRSC shaded relief map of Ganges Mensa (orbit h2211_0000, 7°S/311°E) showing sequences (L1-5) corresponding to thicknesses that were measured (Fig. 53H) along the profile *below*. *(bottom)* Geological profile with sequences deduced from outcrop of the figure *above*. The strike and dip (Fig. 53J) is not considered, therefore layers may dip slightly outward and are not as tilted as shown. However, the top is horizontally layered and layering is traceable all around whereas lower parts and slightly inclined (cf. Fig. 53J) which may be an effect of weathering since the southern part is protected by mantling. Accuracy: Distance ±0.075 km, topography ±12.5 m (HRSC DTM orbit 2211_0000).